R-PLUS: A Riemannian Anisotropic Edge Detection Scheme for Vascular Segmentation

Ali Gooya[1], Takeyoshi Dohi[2], Ichiro Sakuma[1], and Hongen Liao[1,3]

[1] Graduate School of Engineering, the University of Tokyo, The University of Tokyo
[2] Graduate School of Informaiton Science and Technology, The University of Tokyo
[3] Translational Systems Biology and Medicine Initiative, The University of Tokyo
7-3-1, Hongo, Bunkyo, Tokyo, 113-8656
{gooya,ichiro,liao}@bmpe.t.u-tokyo.ac.jp

Abstract. In this paper, detection of edges in oriented fields is addressed. In some applications such as vessel segmentation because of the intrinsic orientation of the structures, edge detection is only demanded in a particular subspace. This is specially usefull when a curve evolution is chosen for segmentation since gradients in parallel to vessel orientation may stop the contour. An anisotropic edge detection scheme is generalized on a Riemannian manifold using the local structure tensor. The method is the generalization of the *PLUS* operator proposed in [8] for accurate curved edge detection. Examples are given and the comparison is made with the state-of-the-art flux maximizing flow which indicates that significant improvements in terms of leakage minimization and thiner vessel delineation is achievable using our methodology.

1 Introduction

Magnetic Resonance Angiography (MRA) is increasingly used to provide volumetric information of vascular system. Accurate assessment of MRA images requires that the vessel structures to be extracted from MRA data sets. Currently, a number of techniques have been developed for vessel segmentation based on the advanced level set evolutionary methods [11,1].

Despite of relative success from some of these methods, segmentation of long thin structures is still considered as a delicate task. Most of these techniques are edge detection based and therefore, their success mainly depends on the accuracy of the detected edges. Classic edge detection methods have shown to produce inaccurate estimation of the edges for curved surfaces (such as blood vessels). Haralick edge detection operator, $I_{\xi\xi}$, [7] defines the edge as a point where the gradient magnitude is maximized along side the image gradient orientation, but under-estimates the actual radius of the curved surfaces. Zero-crossing of Laplacian ΔI or "Marr-Hildreth" [10] edge detection gives an over estimation because of the system point spread function (PSF). Since both $I_{\xi\xi}$ and ΔI appear to be dislocated in opposite direction[9], Verbeek and van Vliet [8] proposed the *PLUS* operator which sums $I_{\xi\xi}$ and ΔI, which improves the accuracy of the edge location an order better.

D. Metaxas et al. (Eds.): MICCAI 2008, Part I, LNCS 5241, pp. 262–269, 2008.

As we will see the original (Euclidean) *PLUS* edge detection has a shortcoming to segment elongated thin vessels. The reason is that *PLUS* edge detector has a isotropic behaviour, meaning that it is equally sensitive to gradients in all orientations. Therefore, in a contour propagation scenario, those noisy image gradients parallel to the main orientation prevent further propagation. In fact, sensitivity is mainly needed across the planes normal to vessel local orientation. This paper proposes a Riemannian generalization of the *PLUS* operator (hereafter called *R-PLUS*) using the local structure tensor which improves the continuity of the extraced vessels. A simple form of such a tensor is given and illustrated using an example and a few TOF-MRA data sets.

1.1 Related Work

For segmentation of thin structures, Gazit *et al.*[3] proposed a combinational curve evolution method, using Haralick edge detector and Chan-Vese minimal variance functional and geodesic active contours. Our methodology is different from that model, since we utilize local structure information for edge detection, and the method does not depend on GAC or Chan-Vese model. Flux maximizing flow was introduced by Vasilevsky [2] that integrates the directions of gradient vectors into the evolution equation so that the gradient flux through the evolving curve is maximized (here after called FLUX). With respect to the authors, we show that in fact since the FLUX is basically a Marr-Hildreth kind of edge detection scheme, it usually overestimates vessel widths (particularly in thinner vessels with high isophote curvature) while using our method more accurate segmentation is achieved in lower contrast thin vessels.

2 Basic Edge Detection Schemes

Zero crossing of Laplacian ΔI was proposed by Marr-Hildreth in [10] as an edge detector. Haralick edge detector [7]finds the image locations where $|\nabla I|$ has a local maximum along the gradient. In other word, edge is defined as a point where the directional derivative of $|\nabla I|$ along side $\boldsymbol{\xi} = \frac{\nabla I}{|\nabla I|}$, i.e, $I_{\xi\xi}$ is zero:

$$\nabla|\nabla I|.\boldsymbol{\xi} = 0 \tag{1}$$

This implies that the inside the object $\nabla|\nabla I|.\boldsymbol{\xi}$ is negative and the outside positive. Both Haralick and Marr-Hildreth edge detection schemes suffer from dislocation error in identifying curved edges. Since dislocations from these schemes are in opposite directions, Verbeek et al [8] proposed zero crossing of the summation: $\Delta I + I_{\xi\xi}$ (the *PLUS* operator) for edge detection and achieved better accuracy. This corresponds to an energy functional consisting of two components: the first one minimize (maximize the norm) the outward flow of the image gradient field on the object border, and the second one minimizes the a regional integral, summing values of $\nabla|\nabla I|.\boldsymbol{\xi}$ inside the object. In the next section, these functionals are generalized on a Riemannian manifold.

3 Riemannian *PLUS* Edge Detector

Assume for a given open region D, the evolving surface is represented as the zero level of the level set function $\phi(x)$ where $\phi(x) < 0$ for inside of the object, and $\phi(x) > 0$ for outside. $H(x)$ and is representing Heaviside function such that $H(x) = 1$ if $x \geq 0$ otherwise $H(x) = 0$. Also $\delta(x) = \frac{d}{dx}H(x)$ is the Dirac delta function. Further, assume that M is the Riemannian manifold defined on D and endowed by the metric $g = \{g_{i,j}\}$ [4]. The generalization of *PLUS* operator to M is straight forward. All Euclidean gradient $\nabla(.)$ vectors are transformed to: $\nabla_g(\cdot) = g^{-1}\nabla(\cdot)$. Considering the fact that dot product under the space metric is now defined as: $< \boldsymbol{x}, \boldsymbol{y} >_g = \boldsymbol{x}^t.g.\boldsymbol{y}$ and taking care of all the quantities involved in terms of the metric g such energy functional can be written as:

$$E = \int_M \delta(\phi)\nabla_g^t I.g.\nabla_g\phi + \int_M H(-\phi)\nabla_g^t \| \nabla_g I \|_g.g.\frac{\nabla_g I}{\| \nabla_g I \|_g} \tag{2}$$

where ∇_g and $\| \cdot \|_g$ denotes the gradient and the norm on the manifold. The first term is in fact a line integral measuring the flux on the object border and the second term is the regional term. Minimization of this regional functional implies negative Riemannian dot product operator employed in the equation (1) inside the object, and maximizing the (norm) of *geodesic* flux on the border. Using co-area formula equation (2) can be written as:

$$\int_D \delta(\phi)\nabla_g^t I.g.\nabla_g\phi|g|^{1/2}dx + \int_D H(-\phi)\nabla_g^t \| \nabla_g I \|_g.g.\frac{\nabla_g I}{\| \nabla_g I \|_g}|g|^{1/2}dx \tag{3}$$

in which $|g|$ denotes the determinant of the metric. Considering the fact that $\| \nabla_g I \|_g = \| \nabla I \|_{g^{-1}}$, (3) can be simplified as:

$$E = \int_D \delta(\phi)\nabla^t I.g^{-1}.\nabla\phi|g|^{1/2}dx + \int_D H(-\phi)\nabla^t \| \nabla I \|_{g^{-1}}.g^{-1}.\frac{\nabla I}{\| \nabla I \|_{g^{-1}}}|g|^{1/2}dx \tag{4}$$

In which the gradient vectors appear in Euclidean version. It is easy to see that the Euler-Lagrangian minimizing equation of (4) is as follows :

$$\frac{\partial\phi}{\partial t} = \delta(\phi)[div(|g|^{1/2}g^{-1}\nabla I) + \nabla^t \| \nabla I \|_{g^{-1}}.g^{-1}.\frac{\nabla I}{\| \nabla I \|_{g^{-1}}}|g|^{1/2}] \tag{5}$$

Using Libnitz formula this can be rephrased as:

$$\frac{\partial\phi}{\partial t} = \delta(\phi)[div(|g|^{1/2}g^{-1}\nabla I) - 0.5 \| \nabla I \|_{g^{-1}}\ div(\frac{|g|^{1/2}g^{-1}\nabla I}{\| \nabla I \|_{g^{-1}}})] \tag{6}$$

Let us have a closer look at (6). The first term computes the g-Laplacian of the projected image gradient and it has high responses if ∇I has large components in parallel to main eigen vector of g^{-1}. This is an important property which should be considered in the design of the g, the metric tensor. The second term is the geodesic mean curvature of the image isolevels, and has a similar role

as topological complexity minimizer, i.e., $I_{\eta\eta}$ in the Euclidean version [3]. We observe that for $g = I_d$, (the identity matrix), equation (6) reduces to $\partial\phi/\partial t = \Delta I - 0.5 I_{\eta\eta}$, i.e, the Euclidean *PLUS* operator. However, generalization using the metric tensor g allows a selective behaviour of the edge detection mechanism. All we have to do is to design an appropriate tensor that eliminates the gradient vectors in parallel with main orientation of the local structure.

4 Design of the Metric Tensor

We utilize the structural tensor to define our metric tensor. The local structure tensor at point x can be obtained using the following summation in the neighborhood of $N\{x\}$ [6]:

$$T(x) = \sum_{N\{x\}} \nabla(G_\sigma(x) * I(x))\nabla^t(G_\sigma(x) * I(x)) \tag{7}$$

Where $G_\sigma(x)$ is a Gaussian with a standard deviation σ. Let $0 \leq \lambda_1 < \lambda_2 < \lambda_3$ and $C_i = \boldsymbol{e_i}\boldsymbol{e_i}^t, i = 1, 2, 3$ be the eigen values and their corresponding eigen components of the structure matrix T.

As mentioned in the previous section the tensor g^{-1} should maintain its main components in support of ∇I if it is normal to the local orientation, and in other way the gradients should be eliminated. In this paper we consider a simple form for g^{-1}:

$$g^{-1}(t) = \epsilon(t)C_1 + C_2 + C_3 \tag{8}$$

Where $0 \leq \epsilon(t) \leq 1$ is a decreasing function such that: $\epsilon(0) = 1.0$ which controls the anisotropic behaviour of the tensor. This important property of time-dependency can be explained as follows: in the beginning of the evolution the tensor is isotropic, and all the directions have the same opportunity to be spanned which helps finding the vessel branchings. Anisotropy is increasing in time, and removes the noisy gradients. This behaviour mimics lowering temperature in optimization by simulated annealing and inhibits local minimums.

5 Multi-scale Computation

Multi-scale implementation of (6) can be achieved in a similar way as described in [2]. That means $div(\boldsymbol{v})$ terms are computed as the outward flux of the $\boldsymbol{v}$ on hemo-centric spheres with different radius r and then maximum is chosen over the range of scales:

$$div(\boldsymbol{v}) = \sup_r \{1/N \sum_q \boldsymbol{v}(r\boldsymbol{n}_q).\boldsymbol{n}_q\} \tag{9}$$

Where $\boldsymbol{n}_q$ is unit outward normal vector on the sphere surface. In our implementation N, the number of the sampling points on the sphere is fixed to 24, the range of scales was 0.3, 0.54, 0.99 and 1.6 voxel and entries of $\boldsymbol{v}$ and $\boldsymbol{n}$ with non-integer index, are interpolated linearly.

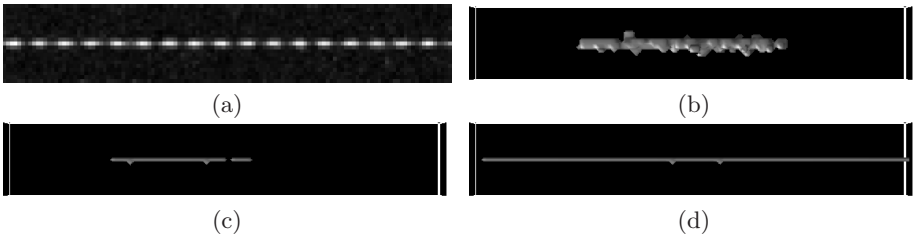

Fig. 1. Riemannian edge detection: (a) Maximum projection image, segmentations obtained from: (b) FLUX, (c) Euclidean PLUS operator ($g^{-1} = I_d$), (d) R-PLUS operator, edges across the model is not detected and a continuous tube is discovered

6 Implementation

In order to have a working contour evolution a few issues must be considered. Since we segment vessels that appear brighter than background, to allow proper vessel edge detection we only allow negative values on the second term in (6). This eliminates the edges resulting from objects with opposite brightness polarity.

A regularized version of delta function,δ_ε is utilized with the same definition as in [5], we used $\varepsilon = 0.5$. Finally smoothness is achieved using minimal surface principle curvature introduced in [**?**]. Therefore using the tensor metric defined in (8), vessel segmentation evolution is as follows:

$$\frac{\partial \phi}{\partial t} = \delta_\varepsilon(\phi)[\nabla.(g^{-1}\nabla I) - 0.5 \parallel \nabla I \parallel_{g^{-1}} S(\nabla.(\frac{g^{-1}\nabla I}{\parallel \nabla I \parallel_{g^{-1}}})) + \alpha \hat{k}] \qquad (10)$$

Where $S(x) = x$ if $x < 0$ otherwise 0. The program is implemented using *Insight Toolkit* and mex library funcitons are called from MATLAB on a Linux system.

7 Synthetic Data Experiment

The maximum intensity projection of a synthetic image is shown in Fig.1.a. We embed a few gap-like signal drop effect along side the model and the target volume is *assumed* to be a straight rod. A Gaussian noise was generated and added with the image. Segmentation using FLUX is shown in panel (b). A few leakage can be observed and the segmented structure appears wider than MIP. Euclidean *PLUS* segmentation is shown in (c) which is insufficient to fully discover the target since it has detected the embedded gaps and contour has been trapped in between. However, *R-PLUS* has successfully passed over the signal droppings and the target has been successfully segmented (d). This is because the edges from those gaps are suppressed by projection through g^{-1}. Meanwhile in contrary to (b), a tighter edges have been obtained across the model, which is closer to the actual edge points of the model.

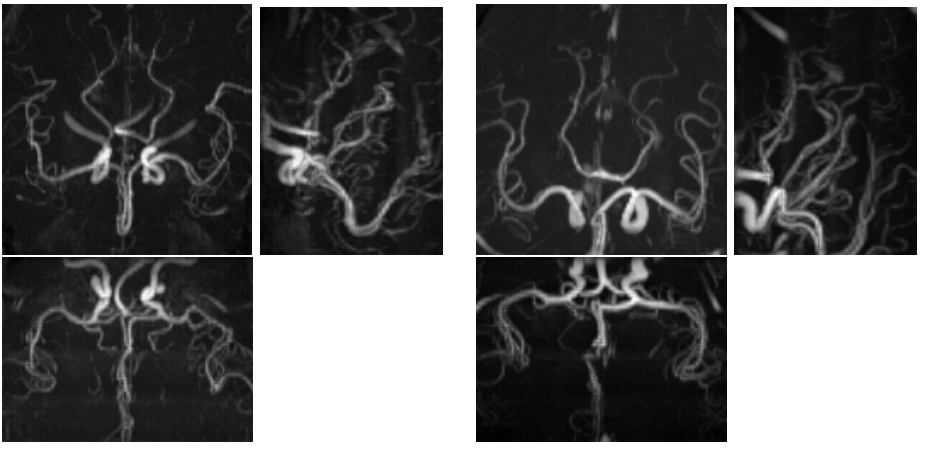

(a) (b)

Fig. 2. MIP images of two 149×149×107 3T TOF-MRA data sets used for segmentation

8 Vessel Segmentation

The efficiency of the proposed edge detection scheme was tested on real data obtained using 3T TOF-MRA protocol. Data sets are randomly chosen from MIDAS Data Server at Kitware, Inc and was resized to a isotropic sampling matrix and then smoothed using a Gaussian smoothing filter with $\sigma = 0.3$ voxel. Segmentation was applied on a selected ROI containing most of vasculatures. Fig.2 indicates the maximum intensity projection of two data sets after smoothing. In these experiments, we set the curvature weight $\alpha = 0.025$. Segmentation result is shown in Fig.3. Initialization was achieved by thresholding the speed image (the right hand side of equation (10)) and intial seeds obtained with the most negative values. Consideration was given to include no seed points outside of vessels. After convergence of isotropic $PLUS$ ($\epsilon(t) = 1.0$) operator, which was obtained after almost 10^3 iterations, the result was feed to $R\text{-}PLUS$ ($\epsilon(t) \simeq 0.0$) and further propagation was observed. This results in detection and merging of some thinner vessels as indicated by arrows in the right column of Fig.3. The result was also compared to FLUX as shown in Fig.4. As it can be observed, vessels are not delineated in the same thickness as they appear in the MIP image (only one volume is shown), and the segmentation includes significant leakage to background area in that term. Similar results has been reported in a recent work in [11].

9 Discussion

In this paper a new Riemannian edge detection scheme was proposed based on the $PLUS$ operator introduced in [8]. Into our knowledge, this extention is new and has not been addressed yet. Also a new level set PDE was proposed for vessel

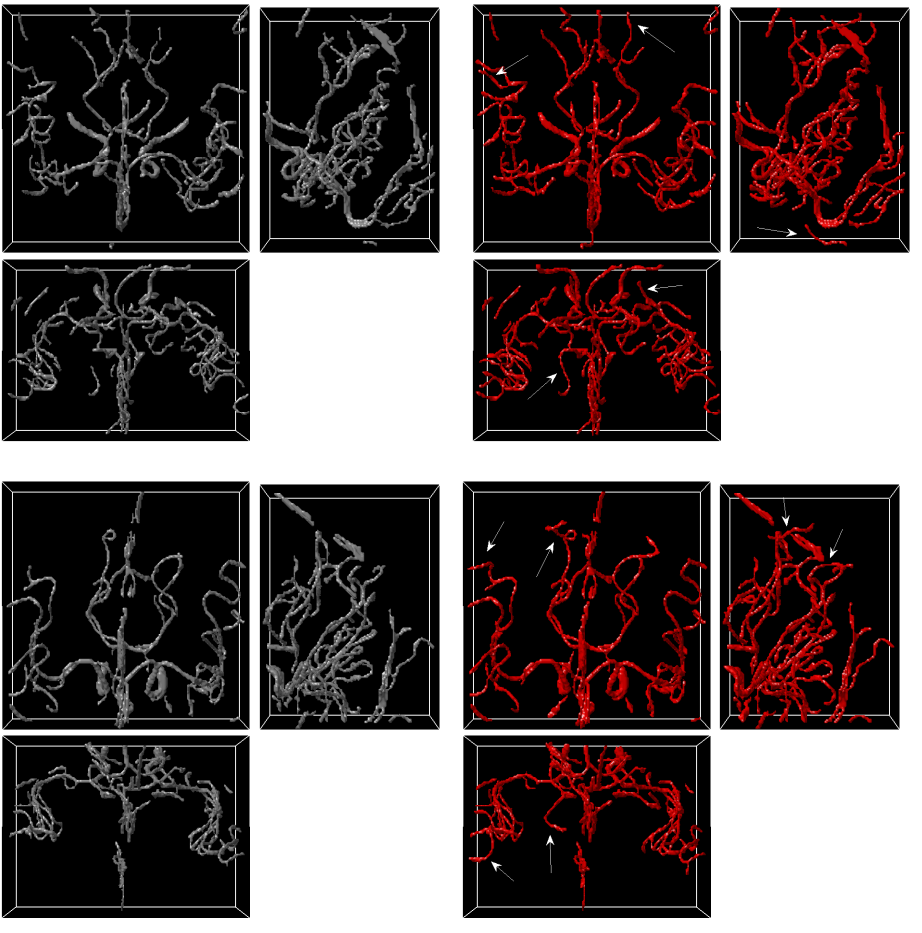

Fig. 3. Segmentations of the first (top) and second (bottom) data sets using: PLUS (left column), R-PLUS (right column). Arrows indicated some vessels that are discovered using R-PLUS.

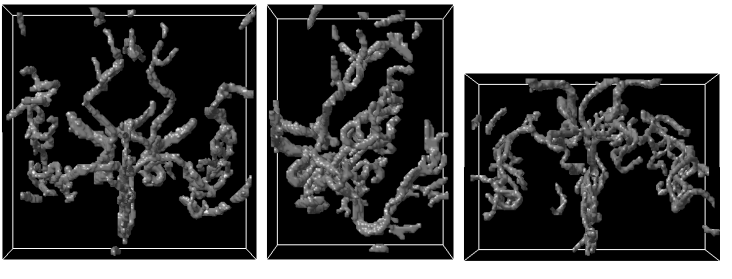

Fig. 4. Segmentation of the first data set using FLUX

segmentation. The tensor metric introduced in this work has a simple form and it can be extended into more complex forms. Yet it is effective and eliminates noisy gradient vectors. The systematic edge detection accuracy problem with similar works [3,2] was addressed and a comparison with standard FLUX method. Our results revealed that the method is able to segment more detailed structures and finer elements. Validation and comparion using other kind of data sets remains as our future research activities.

This study was supported in part by the Special Coordination Funds for Promoting Science and Technology in Japan, and Grant for Industrial Technology Research (07C46050), New Energy and Industrial Technology Development Organization, Japan (both to H. Liao); the Grant-in-Aid for Scientific Research of the Japan Society for the Promotion of Science (17100008 to T. Dohi) and (20.08051 to I.Sakuma).

References

1. Lorigo, L.M., Faugeras, O.D., Grimson, W.E.L., Kerivan, R., Kikinis, R., Nabavai, A., Westin, C.F.: CURVES: Curve evolution for vessel segmentation. Medical Image Analysis 5, 195–206 (2001)
2. Vasilevsky, A., Siddiqi, K.: Flux maximizing geometric flows. IEEE Trans. Pat. Anal. Mach. Intel. 24(12), 1565–1578 (2002)
3. Gazit, M.H., Kimmel, R., Peled, N., Goldsher, D.: Segmentation of thin structures in volumetric medical images. IEEE Trans. Image Proc. 15(2), 354–363 (2006)
4. Shah, J.: Riemannian Drums, Anisotropic Curve Evolution and Segmentation. In: Nielsen, M., Johansen, P., Fogh Olsen, O., Weickert, J. (eds.) Scale-Space 1999. LNCS, vol. 1682, pp. 129–140. Springer, Heidelberg (1999)
5. Chan, T.F., Vese, A.: Active contours without edges. IEEE Trans. Imag. Proc. 10, 266–277 (2001)
6. Weickert, J.: Coherence-enhancing diffusion filtering. Inter. Journal of Computer Vision 31, 111–127 (1999)
7. Haralick, R.: Digital step edge from zero crossing of second directional derivatives. IEEE Trans. Patt. Rec. Mach. Vis. 1(1), 58–68 (1984)
8. Verbeek, P.W., van Vliet, L.J.: On the location error of curved edges in low-pass filtered 2D and 3D images. IEEE Trans. Patt. Rec. Mach. Vis. 16(7), 726–733 (1994)
9. Bouma, H., Vilanova, A., van Vliet, L.J., Gerritsen, F.A.: Correction for the dislocation of curved surfaces caused by the PSF in 2D and 3D images. IEEE Trans. Patt. Rec. Mach. Vis. 27(9), 1501–1507 (2005)
10. Marr, D., Hildreth, E.: Theory of Edge Detection. A Computational Approach to Edge Detection. Proc. Roy. Soc. Lond. B 207, 187–217 (1980)
11. Law, M.W.K., CHung, A.C.S.: Weighted local variance-based edge detection and its application to vascular segmentation in Magnetic Resonance Angiography. IEEE Trans. Imag. Proc. 26(9), 1224–1241 (2007)